Astron. Astrophys. 345, 203–210 (1999)

ASTRONOMY AND ASTROPHYSICS

Interferometric insight into γ Cassiopeiae long-term variability

P. Berio[1], **Ph. Stee**[1], **F. Vakili**[1], **D. Mourard**[1], **D. Bonneau**[1], **O. Chesneau**[1], **N. Thureau**[1], **D. Le Mignant**[2], **and R. Hirata**[3]

[1] Observatoire de la Côte d'Azur, Département Fresnel, CNRS UMR, F-06460 Saint Vallier de Thiey, France
[2] Observatoire de Grenoble, BP53X, F-38041 Grenoble cedex 9, France
[3] Department of Astronomy, Kyoto University, Kyoto, 606-01, Japan

Received 9 December 1998 / Accepted 5 February 1999

Abstract. We present spectrally resolved interferometry of the Be star γ Cas in '88, '91, '93 and '94, obtained with the GI2T interferometer. The analysis of high spatial resolution data across the Hα line reveals azimuthally asymmetric variations which are correlated with those of V/R of the Hα profile. This correlation supports a prograde one-armed oscillation precessing in the equatorial disk of γ Cas due to the confinement by a radiative effect. We examine the occurrence of such oscillations in the context of the latitude dependent radiative wind model developed for previous GI2T interferometric observations of this star. We find that this enhanced equatorial density pattern may be located at 1.5 stellar radii from the stellar surface. We follow its possible rotation through the $-99\,\mathrm{km\,s^{-1}}$, $+92\,\mathrm{km\,s^{-1}}$, $+140\,\mathrm{km\,s^{-1}}$ and $+41\,\mathrm{km\,s^{-1}}$ iso-velocity regions which results in approximate stellar longitudes: 224°, 42°, 153,° and 184° for '88, '91, '93, '94 epochs respectively. Thus, γ Cas is the second Be star after ζ Tau for which interferometric observations directly evidence a prograde one-armed oscillations of its equatorial disk.

Key words: techniques: interferometric – stars: circumstellar matter – stars: emission-line, Be – stars: individual: γ Cas – stars: winds, outflows

1. Introduction

Be stars are charaterized by emission lines which originate in a dense, cool, expanding and rotating envelope. Among these stars γ Cas (B0.5e, HD5394, HR264), discovered by Padre Secchi more than one century ago, is the most studied Be star among its class. The detailed physics and geometry of γ Cas envelope have been studied in recent years by optical long baseline interferometry (Stee et al. 1995, Quirrenbach et al. 1997). This envelope is a flattened disk with a major axis of 17 stellar radii (i.e $\sim$ 4 mas) and an axial ratio of 0.72 (see Stee et al. 1995 for more details). More recently, Stee et al. (1998) investigated γ Cas's envelope in the continuum, Hβ, Hα and HeI λ6678 lines. They found that the envelope size increases following the sequence $2.3R_*$ in HeI λ6678, $2.8R_*$ in 480nm continuum, $3.5R_*$ in 650nm continuum, $< 8.5R_*$ in Hβ and $17R_*$ in Hα emitting regions. The striking result of this study is that the HeI λ6678 emitting region is smaller than the overall continuum source.

Whilst the global geometry of Be envelopes seems to be well settled now, the long-term variability in the ratio of the intensities of the violet and red Balmer emission peaks (the so-called V/R variations) could indicate a global modification of γ Cas's envelope geometry. This quasi-periodic V/R variation is characterized by the shift of the whole emission line towards the wavelength of the V or R component which is the weakest (Mc Laughin 1961). γ Cas also keeps these characteristics (Doazan et al. 1983). Mc Laughin argued that this behavior cannot be explained by the expanding/contracting axially symmetric ring (disk) and supported the elliptical ring (disk) with Keplerian motion, which was originally proposed by Struve (1931). The one-armed global oscillation model, where a thin non-self gravitating Keplerian disk is distorted through a density wave (m=1), is a modernized version of this elongated disk and provides the physical basis if the disk obeys Keplerian motion (Kato 1983, Okazaki 1991). The non-spherical potential due to the rotationally flattened central star produces the precession of the global oscillation with periods on the order of ten years (Papaloizou et al. 1992). More recently, Okazaki (1997) found that for Be stars around B0-type it is the radiative effect that is important for the confinement of the one-armed oscillations. The rotational effect plays a minor role for these stars. Based on this model, Telting & Kaper (1994), Hanushik et al. (1995) have examined a global modification of γ Cas's envelope geometry.

The binary model proposed by Harmanec & Kriz (1976) is another view where the companion star deforms the disk into an elliptical disk through tidal interactions. In case of γ Cas, Kubo et al. (1998) have recently interpreted its X-ray characteristics in terms of the accretion disk around a white dwarf based on the ASCA observations, and proposed the binary system with the separation less than $300R_\odot$ and a possible binary periods of 150 days (see also Smith et al. 1998 for another view in terms of stellar corona with magnetically generated structures).

In a recent paper, Vakili et al. (1998) reported the first interferometric detection of a prograde one-armed oscillation in the equatorial disk of the Be star ζ Tau. The present paper aims to study the long-term variation of γ Cas envelope using spectrally resolved interferometry with the GI2T at the Observatoire

Send offprint requests to: P. Berio (berio@obs-azur.fr)

Table 1. Journal of obsevations from 1988 to 1994. B is the projected baseline in meters on the sky plane. The last row corresponds to the observation of the reference star α Cep.

Star	Date	B (in meter)
γ Cas	88/29/12 (T1)	21.05
	91/21/8 (T2)	49.90
	93/8/11 (T3)	20.70
	93/16/11	28.0
	93/24/11	39.8
	93/25/11	51.0
	93/28/11	29.65
	94/5/9	27.7 and 39.6
	94/6/9 (T4)	22.05 and 33.7
	94/7/9	45.5
α Cep	94/7/9	22.05

de la Côte d'Azur in France (Mourard et al. 1994). Although the Keplerian disk has not yet proven directly from our interferometric observations and the binary model cannot be excluded at present, we examine our observational results in terms of one-armed oscillation model, since this model could provide fruitful results as already mentioned.

The following section describes γ Cas observational material for '88, '91, '93 and '94, and their analysis following cross-spectral and spectral density methods (Mourard et al. 1994, Vakili et al. 1997). In Sect. 3, we present the interferometric results and their interpretation in correlation with V/R long term variations of Hα emission profile. In Sect. 4, we discuss the implications of our findings on the two-component radiative wind model proposed for γ Cas by Stee et al. (1995) in relation with the theory of one-armed oscillations of its equatorial disk. Finally, we summarize our conclusions and examine future routes to progress in the understanding of γ Cas and the Be phenomenon in general.

2. Observation and data reduction

The γ Cas observations were carried between 1988 and 1994 using the GI2T interferometer in southern France. The journal of observations is given in Table 1. All baselines are in the north-south direction.

2.1. The cross-spectral data reduction

The cross-spectral method has already been applied for studying the LBV star P Cyg (Vakili et al. 1997). For the present work, the relative phase of the fringe signal between narrow spectral channels across Hα and its neighbouring continuum was computed on an average for bandwidths of $0.4nm$ and $3nm$ respectively. We swept the Hα spectral region from the blue to the red wings by steps of $0.2nm$. We remind that the relative phase measured in this way provides the spatial location (projected on the GI2T North-South baseline) of iso-radial velocity regions emitting at a given Doppler-shift with respect to the γ Cas continuum source. A positive (negative) relative phase indicates the position at the north (south) of the central star. The accuracy of the phase determination which allows to measure a position can be better than the actual resolution of the interferometer, but is restricted to the case where the envelope remains unresolved or partially resolved. Of course the super-resolution power of cross-spectral density method applies as long as the star is partially resolved (Chelli & Petrov 1995). In Fig. 1 we present γ Cas relative phase as a function of Doppler-shift across Hα for different epochs of observation in '88, '91, '93 and '94. The same diagram for the reference star α Cep observed in 1994 is plotted in Fig. 2 showing nearly a constant relative phase independent of the radial velocity and is in agreement with the case of an unresolved objet. The error on phase measurements $\sigma\phi$ is generally dominated by the GI2T's detector geometrical instabilities at its recombined focal plane. In order to give an external error estimate of the relative phase, we have computed its dispersion in continuum/continuum cross-spectra of γ Cas as well as on the reference stars. This error was found to attain $\sigma\phi = 5^\circ$ in general.

2.2. The spectral density data reduction

The spectral density method gives the modulus of the spatial power spectrum of γ Cas once its raw visibilities have been calibrated on a reference source. In practice we normalize Hα visibilities on the visibility of the continuum next to it: a mean to access to the extent of γ Cas at a wavelength with a given spectral bandwidth. Fig. 3 depicts the auto-calibrated fringe visibilities of γ Cas between '88 and '94 at different baselines and taken over a spectral bandwidth of $3.2nm$ corresponding to the total Hα emission. Note that calibrations were also made using continuum bandwidths of $3.2nm$. By inspecting Fig. 3, we note that the visibility curves are flattened for baselines longer than 30m. This suggests that for those baselines, the visibility is dominated by the unresolved photosphere. Indeed, possible changes in the visibility at different epochs can be due to changes in the size of the disk itself or to changes in the equivalent width of the Hα emission line. However, our spectral density data are not accurate enough to disentangle between these two explanations. Therefore, we have decided to interpret γ Cas long term variability from the phase data alone.

3. Interpretation of interferometric measurements

The shape of relative phase diagrams shown in Fig. 1 reveals the kinematics in the equatorial disk of γ Cas. For a rotating-expanding envelope with azimuthal symmetry (Stee 1996), the phase diagram is strictly an odd function of Doppler shift across Hα around the Radial Velocity RV=0 km.s^{-1}. Any deviation from such a shape, e.g. position of the zero phase on the Doppler-shift axis or the difference between the amplitudes of the negative and positive parts of the phase diagram, implies asymmetrical morphological structures in the equatorial disk of γ Cas. This is exactly what is witnessed by the phase diagrams of Fig. 1 for different epochs of GI2T observations: whenever V/R$<$1 (see also Table 2) the zero value of the relative phase

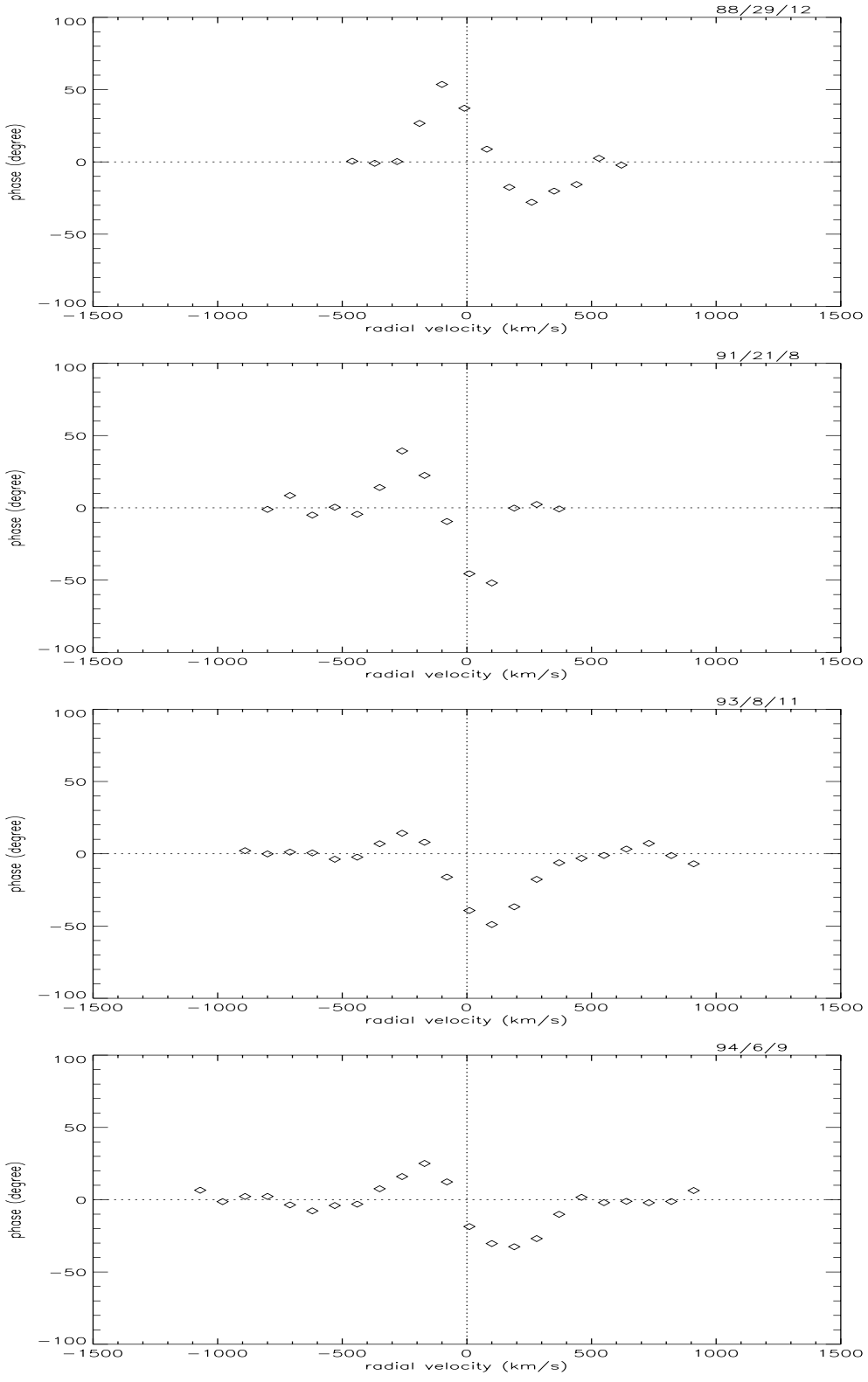

Fig. 1. Relative phase of the interferometric signal as a function of radial velocity across Hα for γ Cas observations: 88/29/12 (B=21.05m), 91/21/8 (B=49.9m), 93/8/11 (B=20.7m) and 94/6/9 (B=22.05m). The error bars are $\pm 2.5^{\circ}$.

occurs at negative radial velocities, whilst for V/R>1 in '88 it occurs at a positive radial velocity.

It is worth carrying out a qualitative comparison of these morphological variations in relation with V/R variations of Balmer line emission profiles. Regular and systematic observations of V/R variations for γ Cas are available in the literature for Hβ only until 1990 (Fig. 4). In order to infer the V/R values at the time of GI2T observations we fit an amplifying-damped sine wave to the values given by Horagushi et al. (1994) from which we extrapolate V/R. We find $V/R_{H\beta} > 1$ between 1985

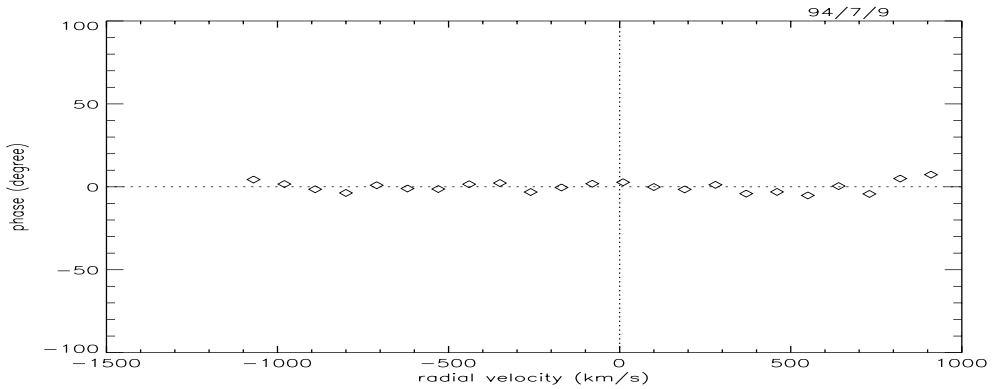

Fig. 2. Relative phase of the interferometric signal as a function of radial velocity across Hα for the reference star α Cep: 94/7/9 (B=22.05m). The error bars are $\pm 2.5^\circ$.

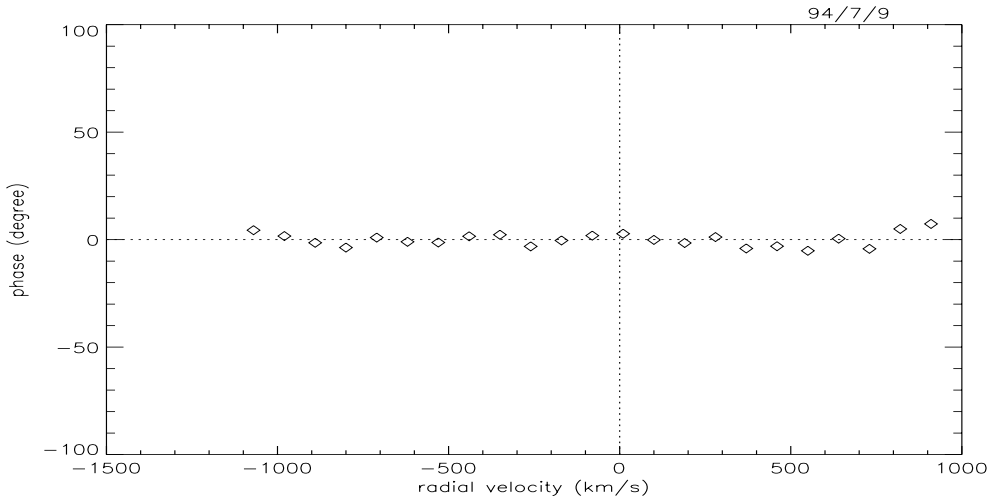

Fig. 3. Modulus of the fringe visibility in Hα normalized by the visibility in the continuum ($\Delta\lambda = 3.2nm$) versus the baselines for the different epochs of observation.

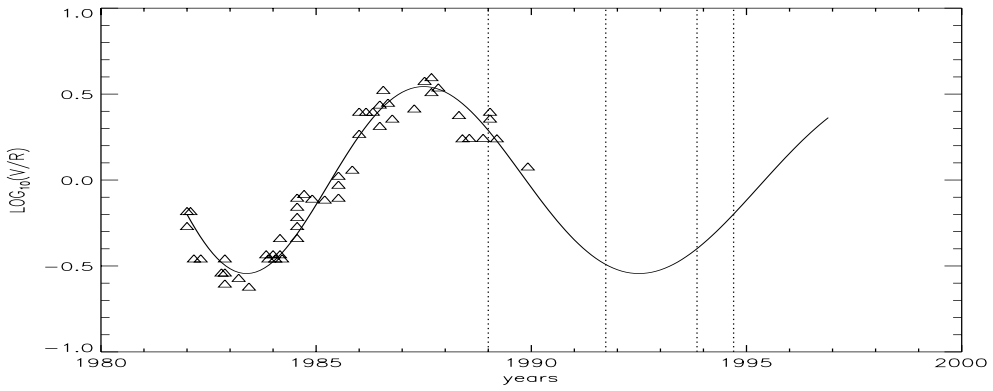

Fig. 4. V/R variations of γ Cas Hβ emission line during the last fifteen years from Horagushi (1994). The solid line corresponds to an amplifying-damped sine wave.

and 1990, and V/R$_{H\beta} < 1$ between 1990 and 1996. Now temporal lags may occur between Hβ and Hα V/R and have been reported for a few Be stars (Kogure & Suzuki 1986), but to our knowledge no such effect occurs for γ Cas. Therefore and in the followings we assume a covariant V/R variations for Hα and Hβ. This hypothesis is confirmed using few low resolution Hα and Hβ spectra obtained with the GI2T (see for instance Fig. 5 in Stee et al. 1995; Fig. 1 in Mourard et al. 1989 and Stee et al. 1998).

Telting & Kaper (1994) have explained the V/R variations of γ Cas as resulting from global one-armed oscillations of its equatorial disk (Okazaki 1991). Such cyclic oscillations create low and high density precessing regions inside the disk with axially symmetrical positions around the central star. According to this picture, the wind particles in the enhanced-density

Table 2. Radial velocity of the zero relative phase for our different observation epochs (T_i).

Observation	Zero phase radial velocity	V/R
T1 (1988)	$+92\,\mathrm{km\,s^{-1}}$	V>R
T2 (1991)	$-99\,\mathrm{km\,s^{-1}}$	V<R
T3 (1993)	$-135\,\mathrm{km\,s^{-1}}$	V<R
T4 (1994)	$-38\,\mathrm{km\,s^{-1}}$	V<R

regions approach the observer for epochs where $V/R > 1$, and recede when $V/R < 1$. In order to compute the center of gravity of given iso-radial velocity regions of the disk (i.e. those parts which emit at a same Doppler-shift across Hα), one must also take into account the perturbations introduced in the density structure patterns. Assuming that these centers of gravity coincide with the photometric centers of emitting regions we can assert that the presence of a high density region shifts the photocenter of the corresponding iso-radial velocity region away from the central star, whereas a low density region shifts the corresponding photocenter towards the central star.

Naturally the location of these photocenters follow the precession of the density patterns explaining the relative phase diagram for the different observations.

For different epochs of GI2T observations we find that the zero of the phase diagrams occur at $+92\,\mathrm{km\,s^{-1}}$ in '88, $-99\,\mathrm{km\,s^{-1}}$ in '91, $-135\,\mathrm{km\,s^{-1}}$ in '93 and $-38\,\mathrm{km\,s^{-1}}$ in '94. In conjunction with the V/R cyclic variability, these radial velocities and their temporal sequence occurrence are consistant with the precession of a low density pattern having precessed in the equatorial disk of γ Cas.

4. One-armed oscillations in the context of Stee & Araùjo radiative wind model

In order to push further our investigation, we hereafter interpret our interferometric evidence of a one-armed oscillations in the context of a radiative wind model. In a recent paper, Okazaki (1997) shows that the radiative effect is the dominant mechanism to confining m=1 oscillations in discs around B0-type Be stars. The rotational effect, as predicted by Papaloizou et al. (1992) coming from the central star's distortion due to its high rotational velocity, is minor for these early type stars. Moreover, Okazaki (1997) studies the confinement of one-armed oscillations by a large number of optically thin lines. In Stee et al. (1995) we also found that, in order to fit our high angular resolution observations and to obtain a $200\,\mathrm{km\,s^{-1}}$ equatorial terminal velocity, the wind in γ Cas equatorial regions must be driven by optically thin lines. Following the parametric form of the radiative force proposed by Chen & Marlborough (1994), the m=1 oscillations require a radiative effect as large as $\eta\epsilon \gtrsim 4.\,10^{-3}$. In our radiative wind model $\eta\epsilon$ is in the range 10^{-1} to 10^{-2}, which is enough to confine the one-armed oscillations in γ Cas equatorial regions.

Therefore henceforth, we suppose that in the inner region of the dense, cool and slowly expanding equatorial region, a one-armed mode is confined within the disk. In this region, as it can be seen in Fig. 5, the kinematics is dominated by the Keplerian rotational velocity field. At first we assume that the perturbation in the disk kinematics does not significantly modify the velocity field of the radiative wind model. We will use this velocity field to determine the absolute location of the density patterns detected in the phase diagrams.

During its precession, the density pattern produced by the one-armed oscillation must cross different iso-velocity regions of the envelope. Due to the fact that our zero relative phase position measurements $+92\,\mathrm{km\,s^{-1}}$, $-99\,\mathrm{km\,s^{-1}}$, $-135\,\mathrm{km\,s^{-1}}$, and $-38\,\mathrm{km\,s^{-1}}$ are related to the location of the low density pattern, we first compute the low density pattern iso-velocity regions which was found respectively at $44^\circ \pm 5^\circ$, $222^\circ \pm 5^\circ$, $333^\circ \pm 5^\circ$ and $4^\circ \pm 5^\circ$. Where the uncertainty in the longitude pattern location of $\pm\,5^\circ$

Table 3. Position of the high density pattern for our different observation epochs

Observation	High density pattern longitude	Projected velocity	V/R
T1 (1988)	$224^\circ \pm 5^\circ$	$-99\,\mathrm{km\,s^{-1}}$	V>R
T2 (1991)	$42^\circ \pm 5^\circ$	$+92\,\mathrm{km\,s^{-1}}$	V<R
T3 (1993)	$153^\circ \pm 5^\circ$	$+140\,\mathrm{km\,s^{-1}}$	V<R
T4 (1994)	$184^\circ \pm 5^\circ$	$+41\,\mathrm{km\,s^{-1}}$	V<R

In Fig. 6, we plot the projected velocity of a high density pattern at 1.5 R_* from the stellar surface (the "sine wave" shape), from the model by Stee et al. (1995), as a function of the stellar longitude ($0^\circ$is assumed to be on the line of sight of the observer and the central star). Since the high density pattern is symmetrically opposed (i.e at 180° with respect to the star) to the low density pattern, we find that for the stellar longitudes $224^\circ \pm 5^\circ$ (T1:1988), $42^\circ \pm 5^\circ$ (T2:1991), $153^\circ \pm 5^\circ$ (T3:1993), $184^\circ \pm 5^\circ$ (T4:1994), the corresponding iso-radial velocities are respectively $-99\,\mathrm{km\,s^{-1}}$, $+92\,\mathrm{km\,s^{-1}}$, $+140\,\mathrm{km\,s^{-1}}$ and $+41\,\mathrm{km\,s^{-1}}$ (see Table 3).

In order to test the effect of changing the location of the density pattern, we have modified its distance from the stellar surface, starting from 0.5 to 5.0 R_*. For all the distances other than 1.5 R_* it was not possible to find solutions that follow both the phase of the visibility and the Hα V/R.

If we assume that the precession velocity is constant between two observations, we find that the pattern rotation period is increasing from 5.3 to 7.4 and 7.9 years. At first order it is consistant with the mean value of 7 years found by Hirata & Hubert-Delplace (1981). Nevertheless, this increasing period can be due to an outward shift of the precessing pattern. This effect has been foreseen by Papaloizou et al. (1992) who predict that the pattern period could increase as $r^{7/2}$, which implies in our case that the pattern has shifted outwards by less than one stellar radius from 1988 to 1994.

In order to test the influence of the one-armed oscillations on the velocity fields we have computed the iso-velocity regions including the perturbation of the angular and radial components of Okazaki's model for γ Cas.

Thus we used:

$$v_r\,(r,\theta,\phi) \;=\; V_o(\theta) + [V_\infty(\theta) - V_o(\theta)]\left(1 - \frac{R}{r}\right)^{\gamma} + \Delta V_r(r,\phi) \qquad (1)$$

$$v_\phi\,(r,\theta,\phi) \;=\; \chi\left(\frac{GM(1-\Gamma)}{R}\right)^{1/2} sin\theta\left(\frac{R}{r}\right)^{1/2} + \Delta V_\phi(r,\phi) \qquad (2)$$

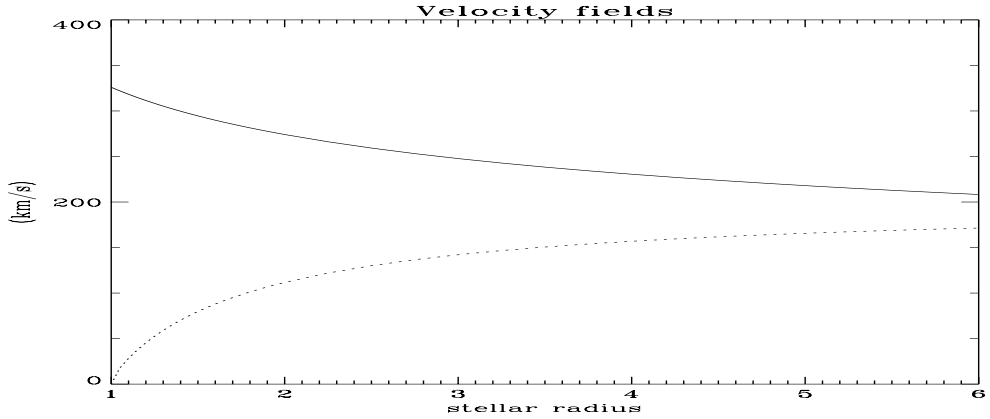

Fig. 5. Velocity fields (in $\mathrm{km\,s^{-1}}$) as a function of stellar radius used in the model developed by Stee et al. 1995 for γ Cas. Thick line: rotational velocity field (Keplerian), dotted line: expansion velocity field.

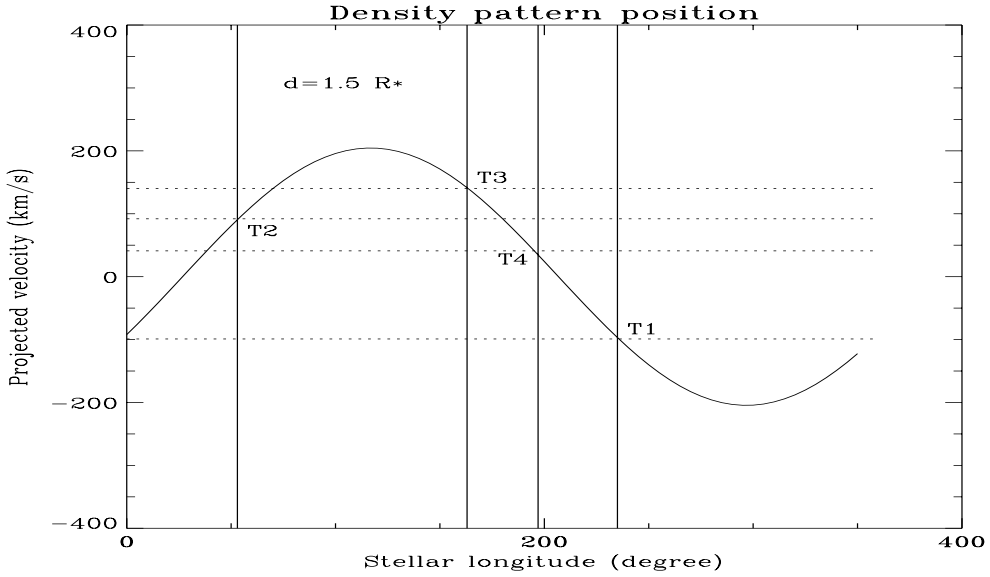

Fig. 6. Projected velocity of a circumstellar region at 1.5 R_* from the stellar surface as a function of the stellar longitude (0°is supposed to be in front of the observer). The horizontal dotted lines are the velocities $-99\,\mathrm{km\,s^{-1}}$, $+92\,\mathrm{km\,s^{-1}}$, $+140\,\mathrm{km\,s^{-1}}$ and $+41\,\mathrm{km\,s^{-1}}$ of the regions with the high density pattern. The vertical lines are the longitude of this pattern for the '88 (T1):224°, '91 (T2):42°, '93 (T3):153° and '94 (T4):184° observations respectively.

where the left part of Eq. (1) and Eq. (2) is taken from Stee et al. (1995) and the perturbation (right part of Eq. (1) and Eq. (2)) is taken from Okasaki's one-armed oscillations calculation.

From Fig. 7 it can be seen that the perturbation modifies slightly the projected velocity field. For instance, the dashed line with the density pattern located at a stellar longitude of 42 ° decreases the projected velocity by $60\,\mathrm{km\,s^{-1}}$ at a stellar longitude of 150 °. The global "sine wave" shape is unchanged and thus the global period of the oscillation remains about 7 years. For the stellar longitudes determined without any perturbation (see Table 3) the changes in projected velocities are less than $10\,\mathrm{km\,s^{-1}}$. Neveretheless the fact that the density perturbation position around the star did not change drastically our results indicates that the exact location of the pattern is out of reach of this study. In that context the conclusion about our possible detection of a precession period increase may not be very clear. We have to compute the Hα line profile, the intensity maps and thus the visibility in modulus and in phase as a function of the pattern position if we want to obtain strong constraints on its exact positions.

Fig. 8 is a top-view representation of γ Cas one-armed precessing oscillations, confined in its equatorial plane at 1.5 R_* according to GI2T observations. The longitude of the pattern is indicated for different observation epochs.

5. Conclusion and discussion

After ζ Tau (Vakili et al. 1998), γ Cas is the second Be star for which interferometric observations evidence the presence of a slowly prograde rotating density pattern in the star's equatorial disk. This prograde precesssion agrees with the Okazaki's model (1997) of the one-armed (m=1) oscillation confined by the radiative effect. We have investigated the possibility of such oscillation to occur within the equatorial regions of a latitude dependent radiative wind model developed by Stee & Araújo (1994). In this model the star is rotationally distorted due to its high rotation. The centrifugal force makes the effective gravity and the brightness temperature decrease from pole to equator and thus the corresponding radiative force will depend on the stellar latitude. Finally the star has a fast wind of high ionization in the polar regions and a slow wind of low ionization, with a high density near the equator. In the inner ($\leqq 10R_*$), cool, dense equatorial regions the kinematics is dominated by the Keplerian rotation, the radiative wind is due to optically thin lines and thus the one-armed oscillations develop. In order to determine

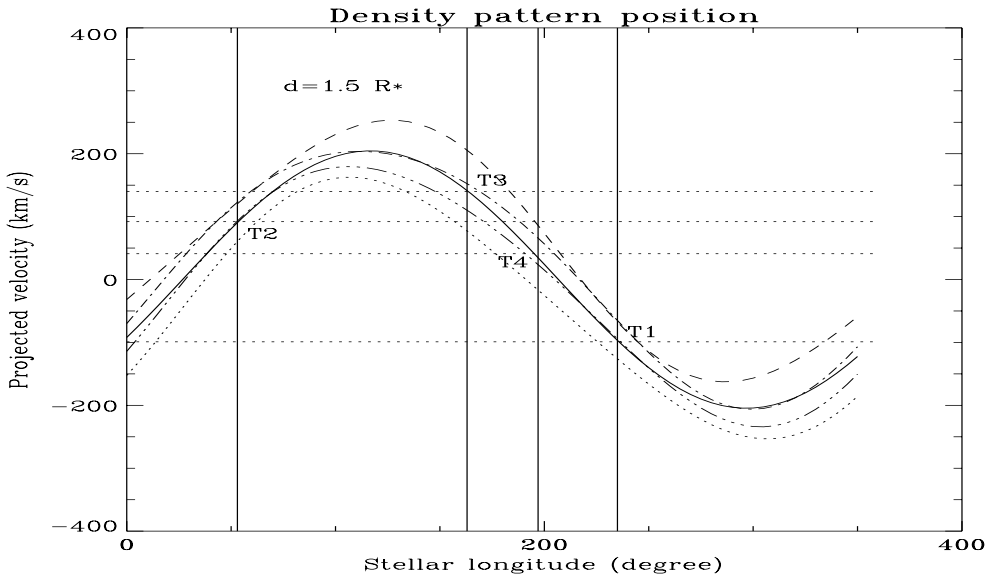

Fig. 7. Thick line: projected velocity of an unperturbed circumstellar region at 1.5 R_* from the stellar surface as a function of the stellar longitude (0°is supposed to be in front of the observer). The horizontal dotted lines are the velocities $-99\,\mathrm{km\,s^{-1}}$, $+92\,\mathrm{km\,s^{-1}}$, $+140\,\mathrm{km\,s^{-1}}$ and $+41\,\mathrm{km\,s^{-1}}$ of the regions with the high density pattern. The vertical lines are the longitude of this pattern for the '88 (T1):224°, '91 (T2):42°, '93 (T3):153° and '94 (T4):184° observations respectively. Dotted line: pertubated projected velocity with an oscillation phase = 224°, dashed line: osillation phase = 42 °, dash dot: oscillation phase = 153°, dash dot dot dot: oscillation phase = 184°

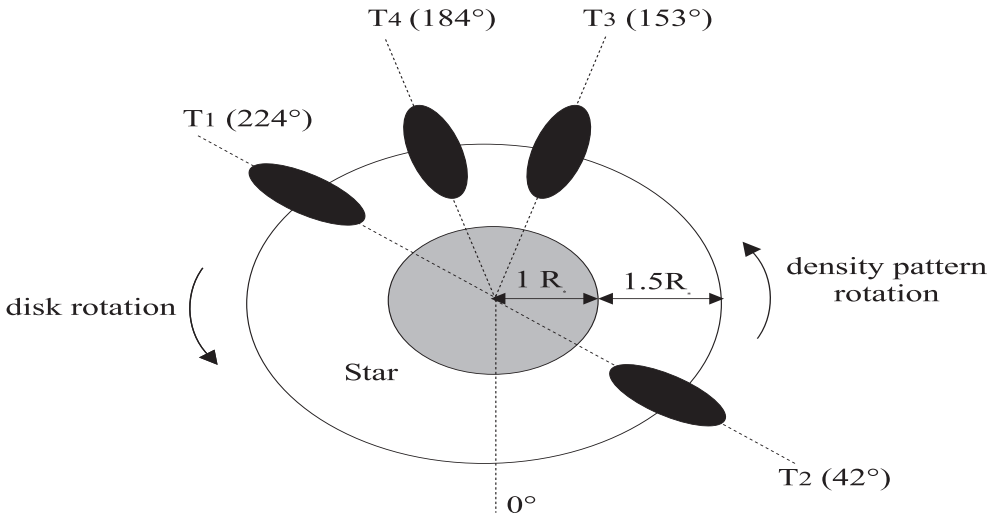

High density pattern in γ Cas equatorial disk

Fig. 8. Schematic representation of γ Cas one-armed precessing oscillations, confined in its equatorial plane at 1.5 R_* according to GI2T observations. The longitude of the pattern is indicated for different observation epochs.

the approximate location of the resulting high density pattern we have followed the iso-velocity regions crossed by the one-armed oscillation. For fitting the visibility phases and the V/R variations of the Hα line profile the high density pattern must be located close to 1.5 R_* and at longitudes 224°, 42°, 153° and 184° in '88, '91, '93, '94 respectively. Finally the mean period of the precession is about 7 years but seems to increase as a function of time, which can be interpreted as an outward shift of the density pattern. In order to test the influence of the one-armed oscillations on the velocity fields we have computed the iso-velocity regions including the perturbation of the angular and radial component from Okazaki's model adjusted to γ Cas. We find minor effects on the projected velocities but substential differences on the longitudes of the high density pattern. Thus, if a prograde precessing pattern at 1.5 stellar radii is detected, its exact position and outward shift remain ambiguous.

Since, we are aware that the present scenario proposed to interpret the long-term variability of γ Cas may not be unique, we hope to obtain a complete simulation of both the Hα line profile V/R variations and the visibility in phase and modulus in the near future. Nevertheless, our interferometric measurements rule out spherical models and our scenario is the first one that agrees well with both spectroscopic and interferometric observations of γ Cas long-term variability.

Acknowledgements. We thank A. Quirrenbach for his constructive refereeing of the paper.

References

Chelli A., Petrov R.G., 1995, A&AS 109, 389
Chen H., Marlborough J.M., 1994, ApJ 427, 1005
Doazan V., Franco M., Rusconi L., Sedmak G., Stalio R., 1983, A&A 128, 171

Hanuschik R.W., Hummel W., Dietle O., 1995, A&A 300, 163
Harmanec P., Kriz S., 1976, In: Slettebak A. (ed.) Be ans Shell stars. IAU Symp. 70, p. 385
Hirata R., Hubert-Delplace A., 1981, In: G.E.V.O.N., Sterken C. (eds.) Workshop on Pulsating B stars. Nice Observatory, p. 217
Horagushi T., Kogure T., Hirata R., et al., 1994, PASJ 46, 9
Huang S.S., 1973, ApJ 183, 541
Kato S., 1983, PASJ 35, 249
Kogure T., Suzuki M., 1984, PASJ 36,191
Kubo S., Murakami T., Ishida M., Corbet R.H.D., 1998, PASJ 50, 417
Mc Laughin D.B., 1961, J. R. Astron. Soc. Can. 55, 73
Mourard D., Tallon-Bosc I., Blazit A., et al., 1994, A&A 283, 705
Mourard D., Tallon-Bosc I., Rigal F., et al., 1994, A&A 288, 675
Mourard D., Bosc I., et al., 1989, Nat 342, No. 6249, 550
Okazaki A.T., 1991, PASJ 43, 75
Okazaki A.T., 1997, A&A 318, 548
Papaloizou J.C., Savonije G.J., Henrichs H.F., 1992, A&A 265, L45
Quirrenbach A., Buscher D.F., Mozurkewich D., et al., 1997, ApJ 479, 477
Smith M.A., Robinson R.D., Corbet R.H.D, 1998, ApJ 503, 877
Stee Ph., de Araújo F.X., 1994, A&A 292, 221
Stee Ph., Vakili F., Bonneau D., et al., 1998, A&A 332, 268
Stee Ph., de Araujo F.X., Vakili F., et al., 1995, A&A 300, 219
Stee Ph., 1996, A&A 311, 945
Struve O., 1931, ApJ 73, 94
Telting J.H., Kaper L., 1994, A&A 284, 515
Vakili F., Mourard D., Bonneau D., et al., 1997, A&A 323, 183
Vakili F., Mourard D., Stee Ph., et al., 1998, A&A 335, 261